

Stretching and bending of line elements in random flows

By I. T. DRUMMOND

Department of Applied Mathematics and Theoretical Physics, University of Cambridge,
Silver Street, Cambridge CB3 9EW, UK

(Received 11 November 1992)

We study the stretching and bending of line elements transported in random flows with known Eulerian statistics in two and three dimensions. By making use of a cumulant expansion for the log-size of material elements we are able to analyse the exponential stretching they exhibit in random flows and identify conditions under which it will and will not occur. The results are confirmed by our numerical simulation.

We also examine the evolution of curvature in material elements and confirm by numerical simulation that it is governed by an appropriate version of the Pope equation. By modelling this equation as stochastic differential equation we are able to explain the appearance of a power-law tail in the probability distribution for large curvature observed by Pope, Yeung & Girimaji (1989) for surface elements. In two dimensions the appearance of the tail can indeed be attributed to the occurrence of events in which the material element undergoes contraction rather than stretching while subject to bending. In three dimensions the relationship between episodes of contraction and strong bending is less direct. This power-law tail allows us to reconcile the observed asymptotic stability, which we confirm here, of the powers and cumulants of the log-curvature with the unboundedness of powers of the curvature itself.

1. Introduction

There has long been interest in the problem of the behaviour of material elements carried along in random flows. The basic processes involved are the stretching, bending and twisting of line and surface elements. These phenomena are closely associated with the problem of non-diffusive mixing of fluids by turbulent flows (Ottino 1989, 1990). One widely recognized criterion for the mixing efficiency of a flow is the exponential stretching of line and surface elements in the flow, an effect first discussed by Batchelor (1952) and subsequently by others (Cocke 1969; Orszag 1970; Kraichnan 1974; Pope 1988; Drummond & Münch 1990). There is also a close connection with the development of flame fronts (Pope 1988; Vassilicos & Hunt 1992), though the superposition of the local flame velocity on the background flow introduces extra complications in this case.

More recently studied is the associated effect of the creation of curvature in material elements (Pope, Yeung & Girimaji 1989; Drummond & Münch 1990, 1991). Mixing after all involves folding as well as stretching and we can expect high curvature to be produced in the hinge of the fold. The nature of the curvature distribution for large curvature should therefore reflect the folding properties of the flow. The ultimate clarification of this point however requires an understanding of the global properties of the flow as well as of the local properties to which we restrict ourselves in this paper. For us the central question is the statistical relationship between bending and

stretching. Pope (1988) analysed this question by means of a relatively simple (Lagrangian) equation for the development of curvature in surface elements. Drummond & Münch (1991) showed that, not surprisingly, a similar equation holds for the development of curvature in line elements. Detailed simulations of the evolution of line and surface elements in random flows have been carried out. A brief summary of relevant results is that exponential stretching is verified and that stretching and bending of material elements occur in distinct regions. An important result is that the mean powers of the curvature increase without limit as time advances. Notwithstanding this result the average value of powers of the log-curvature appear to approach finite limits for large time (Girimaji 1991). The resolution of this seeming contradiction lies in the appearance of a power-law tail in the probability distribution for large curvature (Pope *et al.* 1989). In this paper we re-examine the evolution of both stretching and curvature of line elements in random flows both analytically and by numerical simulation. Of course much of what we say applies also to the motion and evolution of surface elements for which detailed simulations have been carried out by Pope *et al.* (1989) and Girimaji (1991).

Our simulations are based on a velocity field comprising random waves, first introduced by Kraichnan (1970), that we have used in previous work. These model flows are not as realistic as the turbulence model used by Pope *et al.* but have the advantage that their parameters can be varied at will. This makes it possible to check on the operation of the simulation by choosing values that admit theoretical analysis. In particular, by modifying the velocity field appropriately we can demonstrate how long-range correlations can modify the exponential character of the stretching process.

In §2 we briefly recall a few relevant facts about the random velocity field ensemble and give a few details about numerical procedures. We consider the Lagrangian theory of the stretching of line elements in §3 and show how the use of the cumulants of the log-size of the material element provides a clear explanation of the set of exponents, measured previously (Drummond & Münch 1990), that describes the exponential expansion of material elements. The simplest of these exponents is a standard Lyapunov exponent. The higher generalizations have been referred to as Moment Lyapunov exponents by Arnold, Kliemann & Oeljeklaus (1985), who give a rigorous discussion of conditions for their existence. Our discussion is more informal but, we believe, still revealing. We compare the theory with the results of our numerical simulation. In §4 we discuss the Pope equation for the development of curvature in material elements, paying particular attention to the case of two dimensions where the relationship between stretching and bending is especially clear. The analysis is verified by the results from our simulation. In §5 we show how the Pope equation viewed as a multiplicative stochastic differential equation can be modelled in a very simple way leading to a very clear indication that the existence of the probability distribution power-law tail for large curvature is indeed a consequence of events in which the material element shrinks rather than expands. We conclude with a summary and discussion of our results.

2. Random flow model

The model of random flows that we use in this paper was introduced by Kraichnan (1970) and has been described in detail in previous papers, as has the method of simulation (Drummond, Duane & Horgan 1984; Drummond & Münch 1990, 1991).

The velocity field is a sum of modes $v_i(\mathbf{x}, t, \mathbf{k}, \omega, \epsilon)$, where the parameter set $(\mathbf{k}, \omega, \epsilon)$ comprises a wavenumber \mathbf{k} , a frequency ω and a phase ϵ . Thus,

$$u_i(\mathbf{x}, t) = \frac{1}{N^{\frac{1}{2}}} \sum_{n=0}^N v_i(\mathbf{x}, t, \mathbf{k}_n, \omega_n, \epsilon_n). \tag{1}$$

The parameter set in each mode is chosen independently from a predetermined distribution which leads to a velocity field correlation function

$$G_{ij}(\mathbf{x} - \mathbf{x}', t - t') = \langle u_i(\mathbf{x}, t) u_j(\mathbf{x}', t') \rangle$$

of the form

$$G_{ij}(\mathbf{X}, T) = \frac{u_0^2}{D} \left(\delta_{ij} + \frac{k_0^2}{D-1} (X_i X_j - \delta_{ij} X^2) \right) \exp[-\frac{1}{2} k_0^2 X^2] \exp[-\frac{1}{2} \omega_0^2 T^2], \tag{2}$$

where $\mathbf{X} = \mathbf{x} - \mathbf{x}'$ and $T = t - t'$ and D is the dimension of space. We investigate cases with $D = 2$ and 3 . In the above formula u_0 is the r.m.s. velocity, k_0^{-1} is the correlation length and ω_0^{-1} is the correlation time of the velocity field ensemble. For sufficiently large N the statistics of the velocity field are Gaussian so the two-point correlation function given above determines all other correlation functions. For later use we indicate the nature of the approximation to Gaussian statistics in more detail. This can be done conveniently by examining the four-point correlation function. An easily performed classification of the relevant terms arising from the mode expansion yields the result

$$\begin{aligned} & \langle u_i(\mathbf{x}_1, t_1) u_j(\mathbf{x}_2, t_2) u_k(\mathbf{x}_3, t_3) u_l(\mathbf{x}_4, t_4) \rangle \\ &= ((N-1)/N) [G_{ij}(\mathbf{x}_1 - \mathbf{x}_2, t_1 - t_2) G_{kl}(\mathbf{x}_3 - \mathbf{x}_4, t_3 - t_4) \\ & \quad + G_{ik}(\mathbf{x}_1 - \mathbf{x}_3, t_1 - t_3) G_{jl}(\mathbf{x}_2 - \mathbf{x}_4, t_2 - t_4) \\ & \quad + G_{il}(\mathbf{x}_1 - \mathbf{x}_4, t_1 - t_4) G_{jk}(\mathbf{x}_2 - \mathbf{x}_3, t_2 - t_3)] \\ & \quad + (1/N) R_{ijkl}(\mathbf{x}_1, t_1, \mathbf{x}_2, t_2, \mathbf{x}_3, t_3, \mathbf{x}_4, t_4). \end{aligned} \tag{3}$$

There are two kinds of departure from the Gaussian structure. There is a weak breaking represented by the term R_{ijkl} , which vanishes whenever the relative displacement of any two of its arguments is large. This type of term in the cumulant part of the correlation function does not represent a serious departure from Gaussian statistics. It is the kind of term to be expected in more realistic models of random flow. More serious is the strong breaking represented by the coefficient $((N-1)/N)$ multiplying the disconnected terms which yield the Gaussian contribution of the four-point function. The significance of this term not being the full Gaussian term is that it results in an $O(1/N)$ contribution to the cumulant part of the correlation function that is proportional to the disconnected part. It therefore destroys the desirable physical property that two-point correlations measured simultaneously in widely separated regions of the fluid should be independent of one another and identical to the two-point correlator measured on its own. Similar remarks hold for measurements separated in time and space. The strong breaking term therefore represents a long-range effect in both time and space. As such we can expect it to introduce long-range correlations into the Lagrangian statistics of a particle moving with the fluid and indeed we will see evidence for this in our simulation. It is intuitively obvious that this effect is stronger for the higher moments of the velocity field. Indeed it turns out that certain high-order cumulants we compute are sensitive to the number of components

in the velocity field even when N is as large as 100. We will exploit this sensitivity of the model to N in order to demonstrate how long-range correlations may affect higher cumulants.

The Gaussian nature, for sufficiently large N , of the statistics of the velocity field, together with its reliance on a single scale in both time and space means it is not a very realistic model, particularly when compared to grid simulated turbulence models. However the phenomena we are investigating are rather general kinematic processes, the characteristics of which do not seem to depend very strongly on the details of the random flow. Indeed there is a case for supposing that much of what happens to material elements depends on the smallest scale structure of the flow. Under these circumstances the space and time scales in our model can be compared to the corresponding Kolmogorov quantities in more realistic models. Of course large-scale structures may also have an influence on the behaviour of material elements in the flow. Our model can be adapted to incorporate such features although the computational effort is correspondingly greater.

In gathering statistics we found as in previous studies that it was necessary to make use of trajectory samples containing $\sim 5 \times 10^4$ to 2×10^5 particles. Finally we mention that in this simulation we used a fourth-order Runge–Kutta integration procedure which seemed to work well and produce reliable results (Press *et al.* 1986).

3. Stretching

The position vector \mathbf{x} of a particle carried along in the flow field $\mathbf{u}(\mathbf{x}, t)$ satisfies the differential equation

$$\dot{\mathbf{x}} = \mathbf{u}(\mathbf{x}, t). \quad (4)$$

We can generate a curve by making \mathbf{x} depend on a parameter λ . The material line element attached to the particle at \mathbf{x} is $\mathbf{l} = \partial \mathbf{x} / \partial \lambda$. It develops in time according to the differential equation

$$\dot{\mathbf{l}}_i = W_{ij} l_j, \quad (5)$$

where W_{ij} is the velocity gradient tensor. That is

$$W_{ij}(t) = \frac{\partial u_i(\mathbf{x}(t), t)}{\partial x_j}. \quad (6)$$

If we denote the length of the line element by ξ then $\mathbf{l} = \xi \mathbf{t}$, where \mathbf{t} is the unit tangent vector along the curve. The important point for us is that ξ satisfies the Lagrangian equation

$$\dot{\xi} = W(t) \xi, \quad (7)$$

where $W(t) = W_{ij} t_i t_j$. Of course in computing $W(t)$, W_{ij} can be replaced by its symmetric part, the rate of strain tensor. When $W(t) > 0$ the line element is expanding and when $W(t) < 0$ it is shrinking. Because the line element tends to align itself preferentially with the direction of the eigenvector corresponding to the maximum eigenvalue of the rate of strain tensor the mean value of $W(t)$ is positive. However it is a matter of observation in various simulations that $W(t)$ is negative for significant periods. We will see in a later section how this fact can influence the development of curvature. Of course our analysis applies equally well to surface elements although we do not deal with them explicitly in this paper.

It is convenient to set $\xi = \xi_0 e^{\phi(t)}$. The equation for $\phi(t)$ becomes

$$\dot{\phi}(t) = W(t). \quad (8)$$

It has the solution
$$\phi(t) = \int_0^t dt' W(t'), \tag{9}$$

with the result that
$$\xi(t) = \xi_0 e^{\phi(t)} = \xi_0 \exp \left[\int_0^t dt' W(t') \right]. \tag{10}$$

Now
$$\langle \xi(t) \rangle = \langle \xi_0 e^{\phi(t)} \rangle = \xi_0 \exp \left\{ \langle \phi \rangle + \frac{1}{2} \langle \phi^2 \rangle_C + \frac{1}{3!} \langle \phi^3 \rangle_C + \dots \right\}, \tag{11}$$

where $\langle X^n \rangle_C$ denotes the n th cumulant of the variable X . The first term in the exponent on the right-hand side of (11) is

$$\langle \phi(t) \rangle = \int_0^t dt' \langle W(t') \rangle \sim t \Gamma_0 \quad \text{as } t \rightarrow \infty. \tag{12}$$

Here we assume that after the initial conditions are forgotten by the system the statistics of $W(t)$ are time invariant and therefore $\langle W(t) \rangle = \Gamma_0$ where Γ_0 is a constant. In fact Γ_0 is given by

$$\Gamma_0 = \lim_t \frac{1}{t} \log \{ \xi(t) / \xi_0 \}, \tag{13}$$

and so may be identified with the Lyapunov exponent for the line element. The other terms in the exponent in (11) under appropriate assumptions also yield terms linear in t as $t \rightarrow \infty$. From the definition of the cumulant we see that

$$\langle \phi^2 \rangle_C = \int_0^t dt' \int_0^t dt'' F(t' - t''), \tag{14}$$

where $F(t' - t'') = \langle W(t') W(t'') \rangle_C$. From its definition

$$F(t' - t'') = \langle W(t') W(t'') \rangle - \langle W(t') \rangle \langle W(t'') \rangle. \tag{15}$$

At large time separation the values of $W(t')$ and $W(t'')$ are expected to be statistically independent, so that $\langle W(t') W(t'') \rangle = \langle W(t') \rangle \langle W(t'') \rangle$ with the result that $F(\tau) \rightarrow 0$ as $\tau \rightarrow \infty$. Given that there is a Lagrangian timescale characteristic of the fluctuations in $W(t)$ it is reasonable to assume that the quantity γ_2 is finite where

$$\gamma_2 = \int_{-\infty}^{\infty} d\tau F(\tau). \tag{16}$$

It then follows that for large times t ,

$$\langle \phi^2 \rangle_C = \int_0^t dt' \int_0^t dt'' F(t' - t'') \sim \gamma_2 t. \tag{17}$$

Similarly
$$\langle \phi^3 \rangle_C = \int_0^t dt' \int_0^t dt'' \int_0^t dt''' G(t' - t'', t' - t'''), \tag{18}$$

where $G(t' - t'', t' - t''') = \langle W(t') W(t'') W(t''') \rangle_C$. From the definition of the cumulant function we have

$$\begin{aligned} G(t' - t'', t' - t''') &= \langle W(t') W(t'') W(t''') \rangle \\ &\quad - \langle W(t') \rangle \langle W(t'') W(t''') \rangle_C - \langle W(t'') \rangle \langle W(t') W(t''') \rangle_C \\ &\quad - \langle W(t''') \rangle \langle W(t') W(t'') \rangle_C - \langle W(t') \rangle \langle W(t'') \rangle \langle W(t''') \rangle. \end{aligned} \tag{19}$$

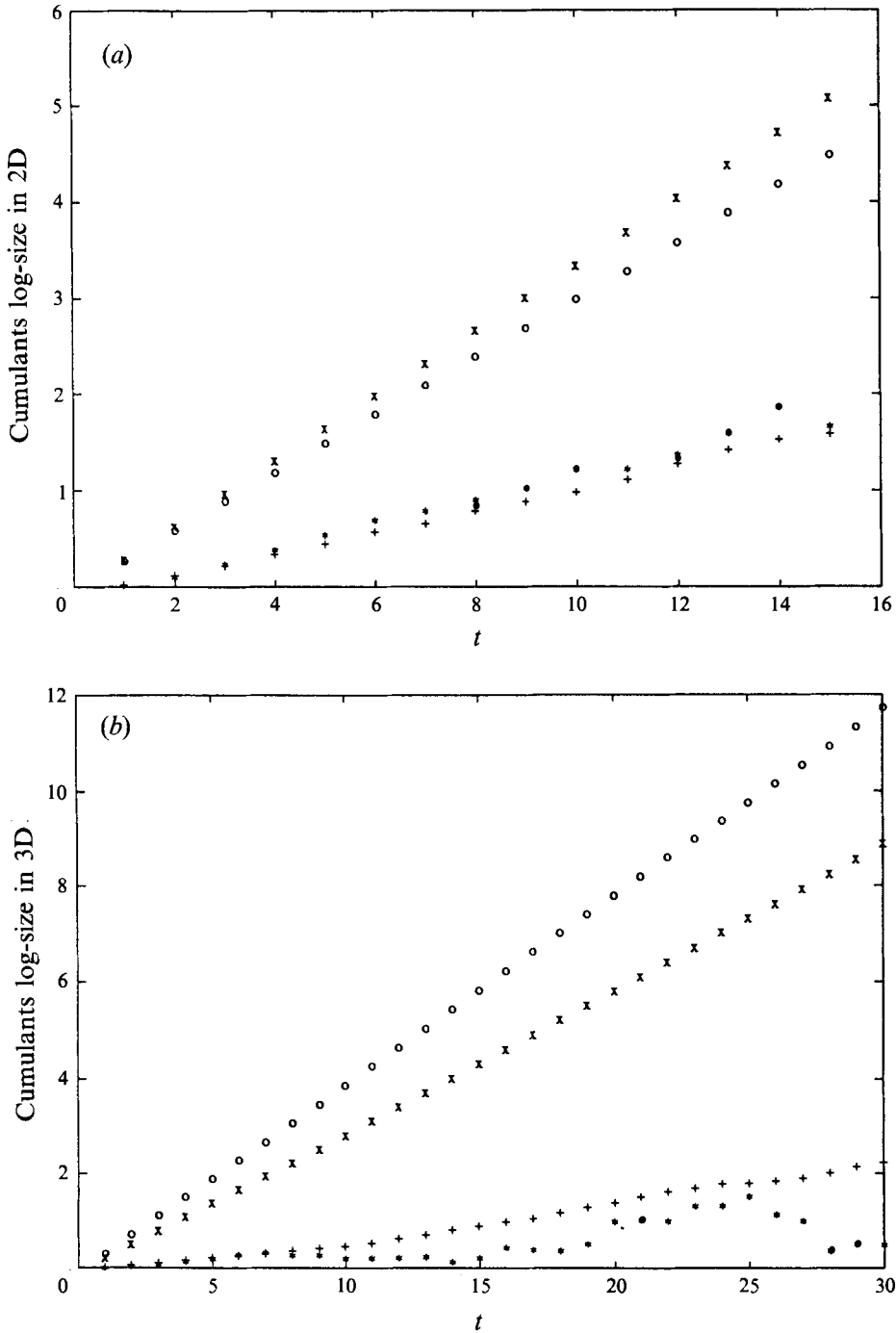


FIGURE 1. The first four cumulants of the log-length for line elements in (a) two dimensions and (b) three dimensions. Model parameters are $k_0 = 1$, $\omega_0 = 1$, $\xi_0 = 1$, $N = 256$ (Gaussian case): ○, first cumulant; ×, second cumulant; +, third cumulant; *, fourth cumulant.

p	$\log(\xi^p)$ (meas.)	$\log(\xi^p)$ (recons.)
-1.0	-2.1687 (16)	-2.149
-0.5	-1.6409 (49)	-1.6453
-0.25	-0.9682 (23)	-0.9683
0.25	1.2859 (27)	1.2859
0.5	2.9189 (77)	2.9173
1.0	7.414 (67)	7.361

TABLE 1. Comparison of values at a given time of moments of the length calculated directly from the simulation and computed from the cumulants according to the theory

The fact that $G(t' - t'', t' - t''')$ depends only on time differences reflects the time independence of the statistics of $W(t)$. It also implies that $G(t' - t'', t' - t''')$ will vanish whenever either or both of its arguments is large. Given the existence of the Lagrangian timescale it is then reasonable to expect that for large times t

$$\langle \phi^3 \rangle_c = \int_0^t dt' \int_0^t dt'' \int_0^t dt''' G(t' - t'', t' - t''') \sim \gamma_3 t, \tag{20}$$

where
$$\gamma_3 = \int_{-\infty}^{\infty} d\tau \int_{-\infty}^{\infty} d\tau' G(\tau, \tau'). \tag{21}$$

Similar reasoning shows that all the higher contributions to the exponent on the right-hand side of (11) exhibit the same kind of asymptotic behaviour for large t . For a general power p we have

$$\langle \xi^p \rangle = \xi_0^p \langle e^{p\phi} \rangle. \tag{22}$$

We can deal with these powers by replacing $W(t)$ by $pW(t)$ in the above analysis with the result that

$$\langle \xi^p \rangle \sim \xi_0^p e^{p\Gamma_p t}, \tag{23}$$

where
$$\Gamma_p = \Gamma_0 + \frac{1}{2}\gamma_2 p + \frac{1}{3!}\gamma_3 p^2 + \dots \tag{24}$$

The simulation was carried out using the methods of previous papers. In figures 1(a) and 1(b) we exhibit the dependence of the first four log-cumulants of the length of the line elements on time in two and three dimensions respectively for the case $N = 256$. Note that the time dependence is indeed linear and that the first two cumulants dominate. In table 1 we compare the expected values at a given time of various moments of the length calculated directly from the simulation with the corresponding quantities computed from the cumulants according to the above theory. The agreement is clearly very close, thus confirming the consistency of the calculation. The dominance of the first two cumulants indicates that the distribution of lengths becomes log-normal to a good approximation, in line with the discussion of Kraichnan (1974) and the results of Pope *et al.* (1989). However the presence of the higher cumulants indicates that there is indeed a departure from log-normality.

The behaviour of the model in three dimensions for the low value $N = 8$ is shown in figure 2. Because the Eulerian statistics of the model are time independent and invariant under spatial translations we expect the Lagrangian statistics to be time invariant also. We should not therefore see any breakdown of the natural cumulant structure at the level of Lagrangian two-point functions. We have no reason to believe

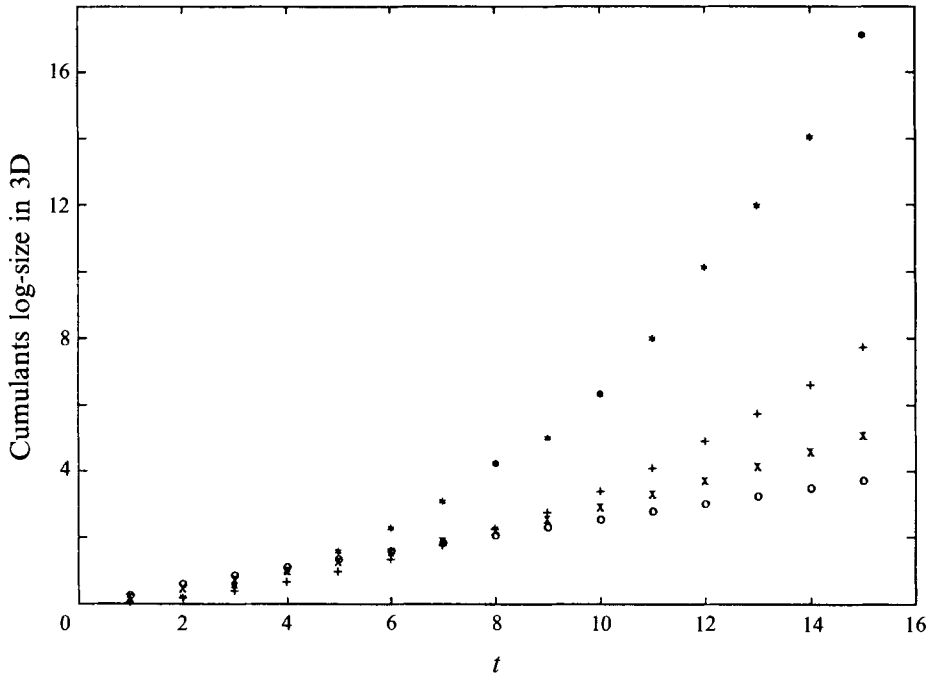


FIGURE 2. The first four cumulants of the log-length for line elements in three dimensions. Model parameters are $k_0 = 1$, $\omega_0 = 1$, $\xi_0 = 1$, $N = 8$ (non-Gaussian case: \circ , first cumulant; \times , second cumulant; $+$, third cumulant; $*$, fourth cumulant).

this will remain true for higher Lagrangian correlations however. Guided by the kind of strong breaking of the Gaussian property we encountered in the Eulerian statistics we might expect the presence for low values of N of terms of the form

$$\langle W(t) W(t') W(t'') \rangle_C \sim (1/N) \langle W(t) W(t') \rangle_C \langle W(t'') \rangle \quad (25)$$

in the cumulant part of the three-point Lagrangian correlation function. Such terms give rise to a time dependence $\langle \phi^3 \rangle_C \sim t^2$. From figure 3 we see that the first two cumulants of the log-length do indeed increase linearly in time though with slopes modified relative to the 'Gaussian case' $N = 256$. For the larger values of t we have, to good accuracy, $\langle \{\phi(t)\}^3 \rangle_C \propto t^2$. For $\langle \{\phi(t)\}^4 \rangle$ we expect from similar arguments contributions to its behaviour of the form $\sim t^2$ and $\sim t^3$. This too is consistent with the results in figure 2.

We feel that this use of log-cumulants in the theory of line (and surface) elements in random flows provides a very clear and natural explanation of the occurrence of exponential growth. Essentially there are two conditions for this to occur, the obvious one of time invariance of the statistics and the more subtle one of rapid time-decorrelation of the rate of stretching function $W(t)$. Indeed if a situation arose in which $W(t)$ exhibited anomalous long-range correlations, not necessarily as gross as those discussed above, that still precluded the convergence of the integrals over the cumulant correlation functions required for the computation of the γ_n then the log-cumulants would no longer develop linearly in time. Correspondingly the average powers of the length would no longer exhibit pure exponential growth. They might well increase faster than exponentially. It would be interesting to explore models with such anomalous behaviour even though we do not expect it to occur in real turbulence.

4. Curvature evolution

In a previous paper Pope (1988) deduced an equation for the evolution of curvature in a surface element. It has the form

$$\dot{\kappa} = -(2W_{ij}e_i e_j - W_{ij}N_i N_j)\kappa + W_{ijk}N_i e_j e_k, \quad (26)$$

where κ is the extrinsic curvature of the surface element associated with the principal direction e_i and N_i is the normal to the surface element. We have used the notation

$$W_{ijk} = \frac{\partial^2 u_i}{\partial x_j \partial x_k}. \quad (27)$$

An equation for the evolution of curvature in line elements was obtained by Drummond & Münch (1991). It has a form very similar to the above, namely

$$\dot{\kappa} = -(2W_{ij}t_i t_j - W_{ijk}n_i n_j)\kappa + W_{ijk}n_i t_j t_k, \quad (28)$$

where we have again used κ for the curvature of the line element, t_i is the tangent vector of the line element and the normal is defined in the usual way as the derivative of the t_i

$$n_i = \frac{1}{\kappa} \frac{\partial t_i}{\partial x}, \quad (29)$$

where s is distance along the curve of which the line element is a part.

Both (26) and (28) have the form

$$\dot{\kappa} = -A(t)\kappa + B(t), \quad (30)$$

where $A(t)$ is computed from the rate of strain tensor and $B(t)$ is computed from its derivative. A formal solution of this equation is

$$\kappa(t) = \exp\left(-\int_0^t dt' A(t')\right)\left(a + \int_0^t dt' \exp\left(\int_0^{t'} dt'' A(t'')\right) B(t')\right), \quad (31)$$

where a is the initial value of the curvature.

It is intuitively clear that $B(t)$, which is associated with the bending properties of the flow, can be viewed as the term which produces curvature in the material elements, while $A(t)$, which is associated with the stretching properties of the flow when it is positive, can act to suppress curvature. It is known that $\langle A(t) \rangle > 0$ so its average effect is indeed suppressive. In this sense the resulting curvature distribution is a competition between the bending and stretching terms in (30). Understanding the nature of the resulting distribution is the central problem of curvature generation in random flows.

The situation is superficially paradoxical in that while various quantities such as powers of the logarithm of the curvature acquire equilibrium values at large times, certain others such as powers of the curvature itself, do not. The former fact suggests that an equilibrium probability distribution for curvature is attained while the latter seems to suggest the opposite. Work by Pope *et al.* (1989) resolved the situation by showing that a power-law tail develops in the distribution. The existence of this tail is associated with the occurrence of events in the history of the material element in which it is subject to bending as a result of the $B(t)$ -term in (30) while undergoing contraction as a result of $A(t)$ acquiring negative values. In this paper we reconfirm the situation just described and present simple models of (30) which show both analytically and through simulation the appearance of the power-law tail in the curvature probability distribution.

Since the two-dimensional situation is particularly simple we will begin with that case. In two dimensions only line elements are of significance for the purposes of

p	a	$t = 0.5\omega_0^{-1}$	$t = 1.0\omega_0^{-1}$	$t = 1.5\omega_0^{-1}$
1	50	-0.3020	-0.8297	-1.304
	100	-0.3014	-0.8220	-1.309
	200	-0.3013	-0.8187	-1.308
	300	-0.3012	-0.8179	-1.307
	500	-0.3012	-0.8171	-1.306
	∞	-0.3012	-0.8170	-1.303
2	50	0.9082	2.611	4.111
	100	0.9059	2.551	4.150
	200	0.9053	2.521	4.143
	300	0.9051	2.513	4.132
	500	0.9051	2.508	4.123
	∞	0.9050	2.504	4.091
3	50	-0.02792	-1.121	-1.829
	100	-0.02160	-7.940	-2.046
	200	-0.02031	-5.929	-2.029
	300	-0.01965	-5.359	-1.956
	500	-0.02023	-4.984	-1.903
	∞	-0.01940	-4.595	-1.612
4	50	0.07877	4.965	6.937
	100	0.06354	3.512	7.719
	200	0.06244	2.256	7.785
	300	0.05933	1.899	7.404
	500	0.06616	1.655	7.279
	∞	0.05803	1.343	4.948

TABLE 2. Comparison between the first four log-cumulants for $\kappa(t)$ and $\xi(t)$ at a sequence of times (the latter indicated by $a = \infty$)

measuring curvature. The relevant equation then is (28). Since the flows with which we are concerned are incompressible we have

$$W_{ii}(t) = W_{ij}(t) t_i t_j + W_{ij}(t) n_i n_j = 0. \tag{32}$$

It follows then from (28) that

$$A(t) = 3W(t). \tag{33}$$

We see therefore that in two dimensions $A(t)$ is indeed very directly related to the stretching of the line element. More precisely the curvature development is related to the third power of the line element. This becomes particularly clear if we use (33) to rewrite (31) in the form

$$\kappa(t) = a \left(\frac{\xi_0}{\xi(t)} \right)^3 + \int_0^t dt' \left(\frac{\xi(t')}{\xi(t)} \right)^3 B(t'). \tag{34}$$

Equation (34) allows us to test the internal consistency of our integration procedures. When a is sufficiently large we can neglect the second term for some initial range of time, with the result

$$\kappa(t) \approx a \left(\frac{\xi_0}{\xi(t)} \right)^3. \tag{35}$$

It follows that in this initial time period the log-cumulants of $\kappa(t)$ are simply related to those of $\xi(t)$. The p th log-cumulant of $\kappa(t)/a$ is $(-3)^p$ times the log-cumulant of $\xi(t)$. For a range of values of the initial curvature a the comparison between the first four log-cumulants for the two sets of quantities at a sequence of times, is exhibited in table 2. The log-cumulants of $\xi(t)$ modified in the appropriate way by the factor $(-3)^p$ are indicated by the choice $a = \infty$. Clearly the agreement is rather good, especially for the

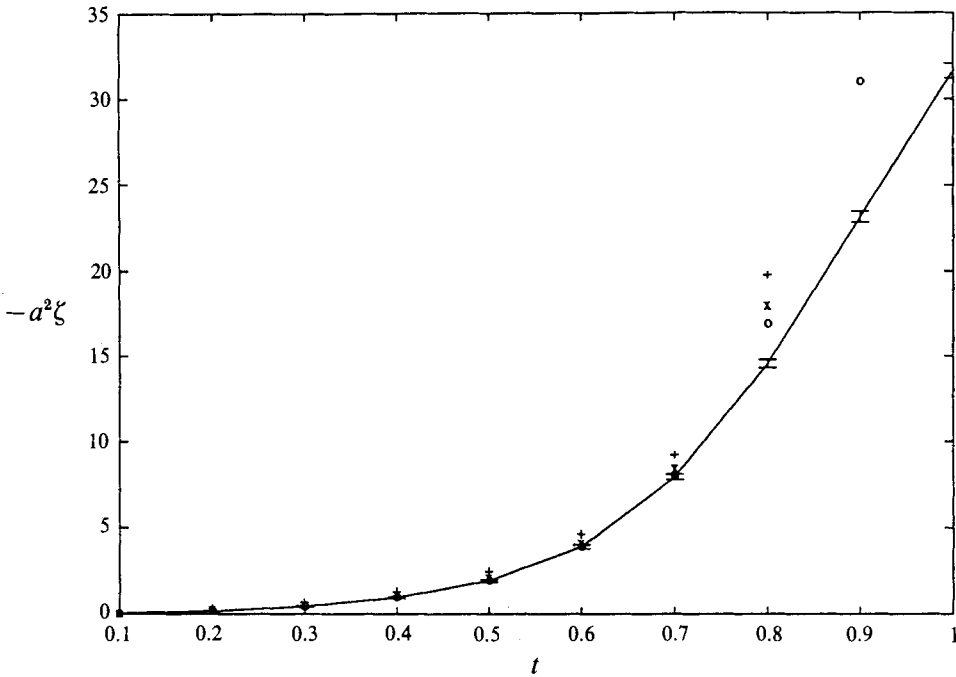


FIGURE 3. The dependence on time t of $-a^2\xi$ for various values of the initial curvature. $+$, $a = 500$; \times , $a = 200$; \circ , $a = 100$; —, $a = 50$.

earlier times and the lower-order cumulants. Note that it is more convenient to compute the log-cumulants rather than simply the powers of the logarithms of the two quantities in order to reveal the relationship between them.

Another test which makes use of (34) is to examine the easily computed quantity ζ , given by

$$\zeta = \log \left(\frac{\kappa}{a} \left(\frac{\xi(t)}{\xi_0} \right)^3 \right). \tag{36}$$

From (34) we see that

$$\zeta = \log \left(1 + \frac{1}{a} \int_0^t dt' \left(\frac{\xi(t')}{\xi_0} \right)^3 B(t') \right). \tag{37}$$

Strictly the argument of the logarithm should be enclosed in modulus signs since as it stands it may be negative as well as positive. However we are interested in situations in which a is very large and positive so the difference will not matter. The issue on which we will focus is the dependence of $\langle \zeta \rangle$ on a . Because expected values of quantities that contain odd powers of $B(t)$ vanish we expect $\zeta \sim O(a^{-2})$. Figure 3 exhibits the dependence of $-a^2\xi$ on time $0 < t < 1$ for a range of values of a . Because of the coincidence of the graphs for the different a -values it is fairly clear that within errors the predicted a -dependence is verified.

If we follow the development of the log-curvature for long periods of time we find that for any initial value of the curvature, they each tend to an asymptotic limit. The magnitude of the limiting value increases rapidly with the order of the cumulant. These higher-order cumulants tend to achieve their limiting value at later times than the low-order cumulants. This is consistent with the results of Girimaji (1991) on the powers of the log-curvature for surface elements. An example of this behaviour for the first six

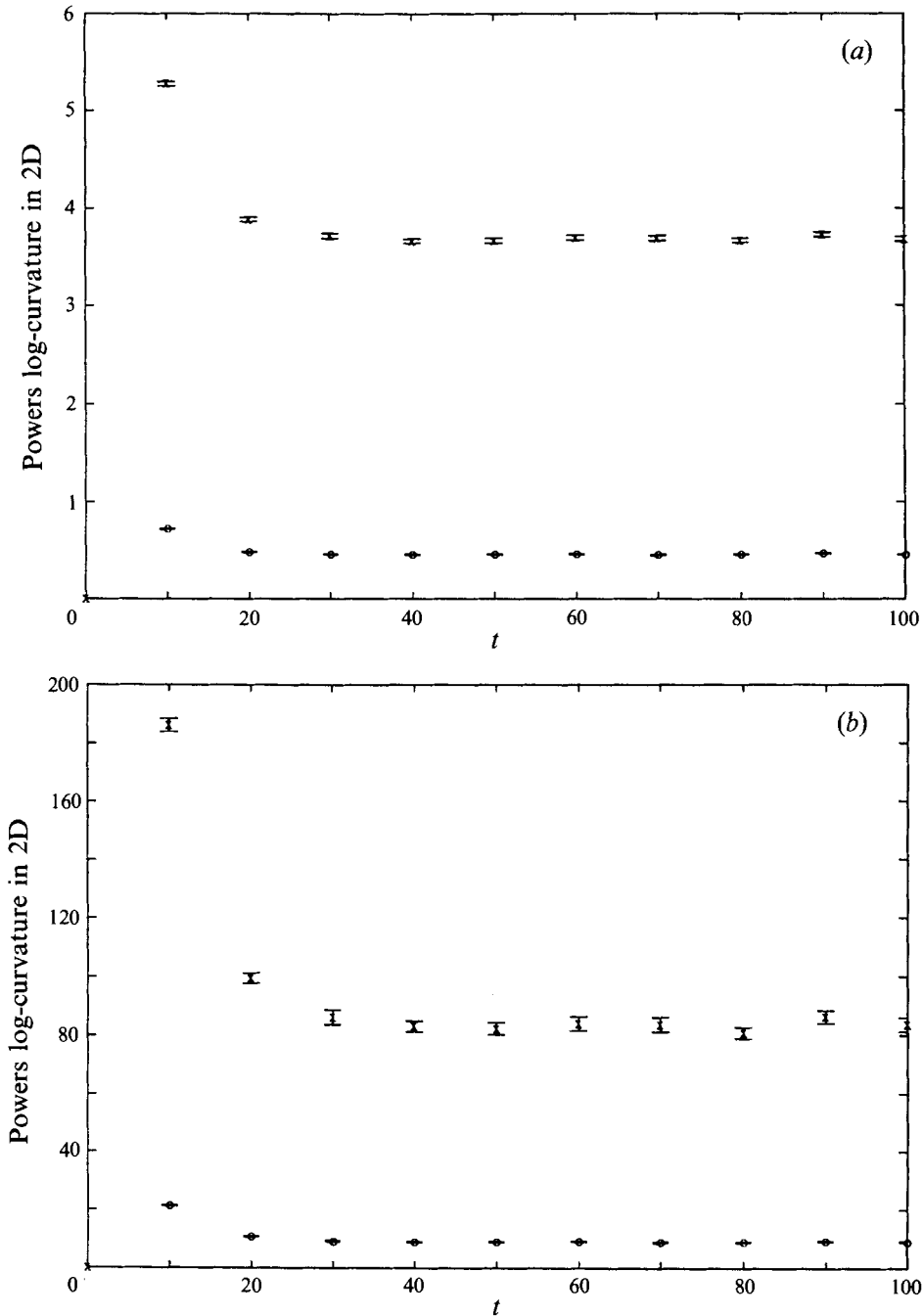


FIGURE 4. For caption see facing page.

moments in the two-dimensional case is shown in figure 4 for an initial value of the curvature of $100k_0$. Identical limiting behaviour for the six moments is observed for zero initial curvature.

For line elements in three dimensions we see from (28) that

$$A(t) = 2W_{ij} t_i t_j - W_{ij} n_i n_j. \tag{38}$$

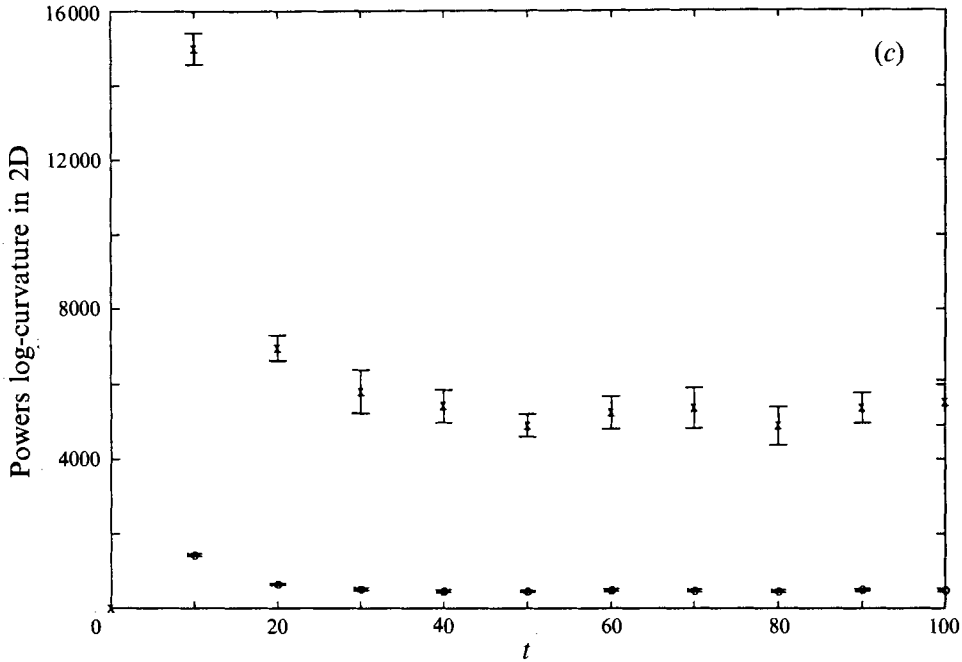


FIGURE 4. The first six powers of the log-curvature as a function of time t in two dimensions. Initial curvature $a = 100$. (a) \circ , first power; \times , second power. (b) \circ , third power; \times , fourth power. (c) \circ , fifth power; \times , sixth power.

t	Order	Cum. log-length	Cum. log-curv.	Ratio	Error
0.1	1	0.00497	-0.00994	2.001	0.005
	2	0.00332	0.0233	7.004	0.0033
0.2	1	0.0194	-0.0388	2.000	0.02
	2	0.0130	0.0910	7.000	0.013
0.3	1	0.0421	-0.0843	2.000	0.045
	2	0.0282	0.197	6.997	0.03
0.4	1	0.0715	-0.143	2.000	0.08
	2	0.0479	0.335	6.995	0.053
0.5	1	0.106	0.212	2.000	0.125
	2	0.0709	0.496	6.991	0.083
0.6	1	0.144	-0.287	2.000	0.18
	2	0.0963	0.673	6.986	0.12
0.7	1	0.183	0.367	2.000	0.24
	2	0.123	0.860	6.980	0.16
0.8	1	0.224	-0.449	2.000	0.32
	2	0.151	1.05	6.972	0.21
0.9	1	0.266	-0.532	2.000	0.405
	2	0.180	1.25	6.964	0.27
1.0	1	0.308	-0.616	2.000	0.5
	2	0.209	1.45	6.954	0.33

TABLE 3. Results of the simulation for the log-cumulants of length and curvature, with $a = 500k_0$

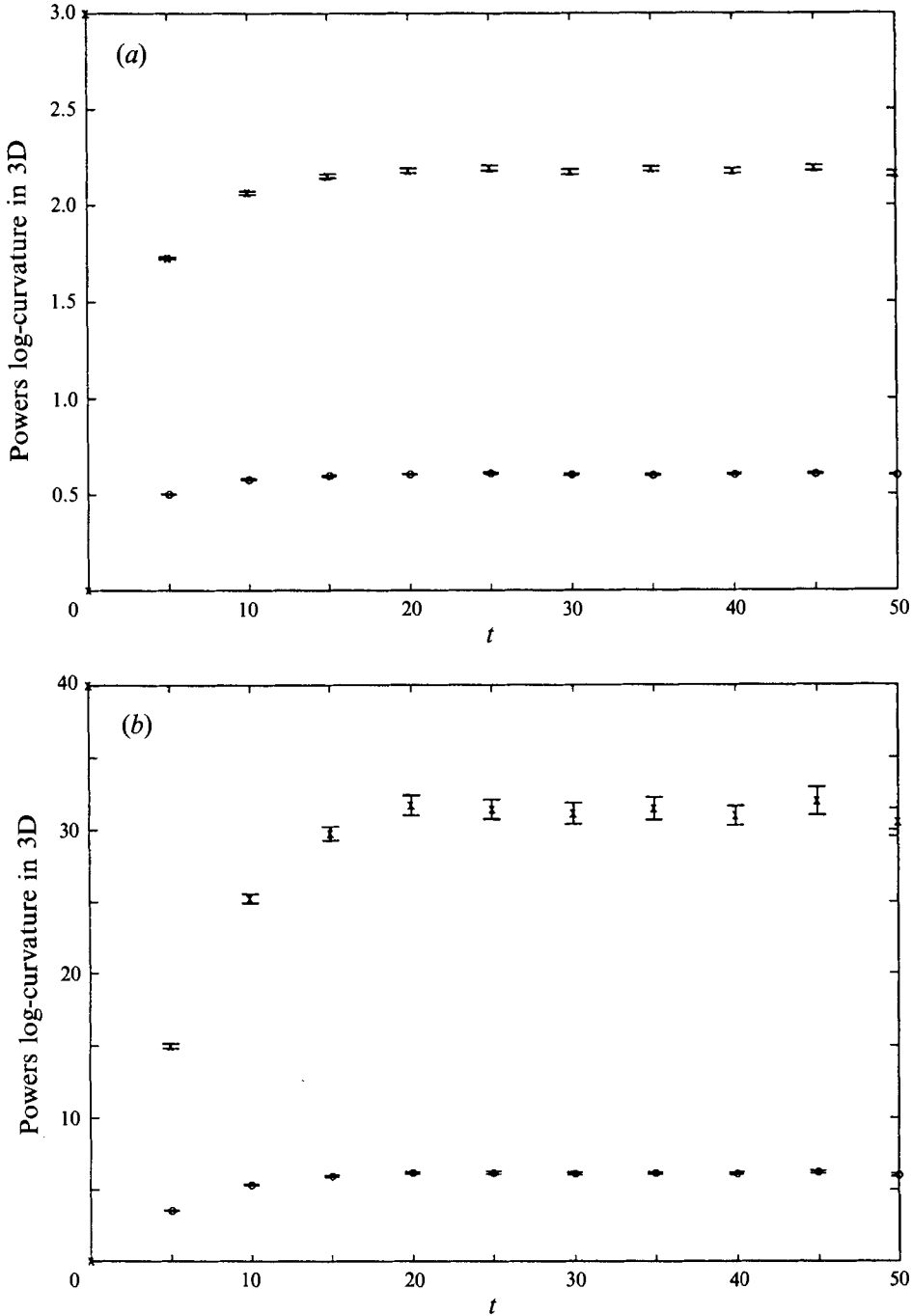


FIGURE 5. For caption see facing page.

If we introduce the bi-normal m_i , orthogonal to both t_i and n_i , we can use the incompressibility of the flow to obtain

$$A(t) = 3W(t) + W_{ij}(t) m_i m_j. \tag{39}$$

In neither (38) nor (39) is the structure of $A(t)$ as directly related to the stretching

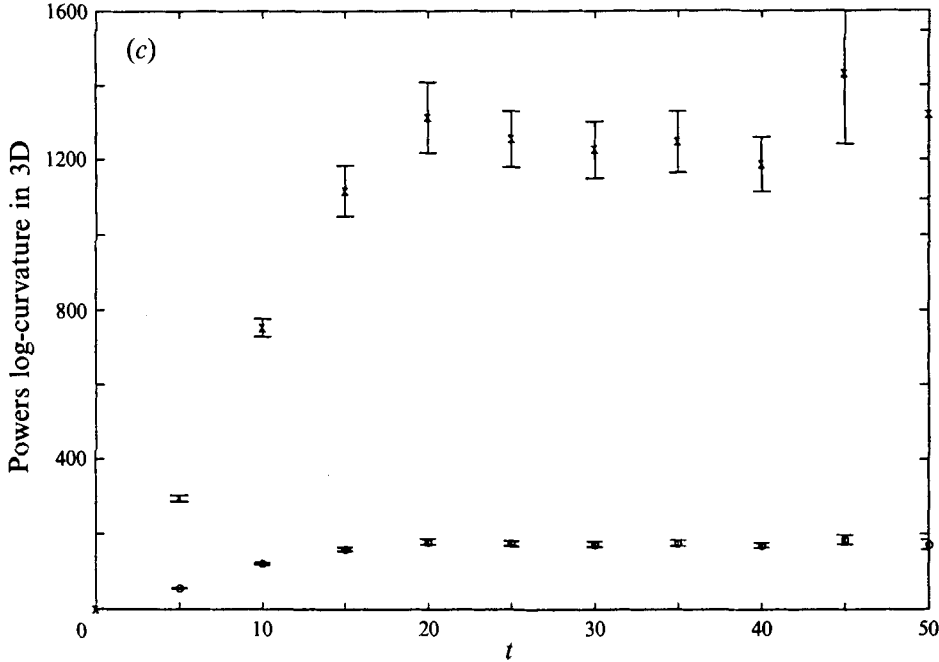


FIGURE 5. The first six powers of the log-curvature as a function of time t in three dimensions. Initial curvature $a = 0$. (a) ○, first power; ×, second power. (b) ○, third power; ×, fourth power. (c) ○, fifth power; ×, sixth power.

coefficient $W(t)$ as it is in the two-dimensional case. This point has also been emphasized by Ishihara & Kaneda (1992). If we examine the behaviour of the contributions to $\langle A(t) \rangle$ for short times, we find to $O(t)$

$$\langle W(t) \rangle = \langle t_i W_{ij} t_j \rangle = \frac{1}{5} \langle W_{ij}(0)^2 \rangle t, \tag{40}$$

and

$$\langle n_i W_{ij} n_j \rangle = 0. \tag{41}$$

This last result implies that for short times we expect from (31) to find that

$$\langle \log(\kappa/a) \rangle = -2 \log \xi = \frac{1}{5} \langle W_{ij}(0)^2 \rangle t^2, \tag{42}$$

the initial curvature a being assumed large. Under the same circumstances we find

$$\langle (\log(\kappa/a))^2 \rangle_c = 7 \langle (\log \xi)^2 \rangle_c = \frac{7}{15} \langle W_{ij}(0)^2 \rangle t^2. \tag{43}$$

In table 3 we show the results of the simulation for these log-cumulants in the time interval $0 < t < 1$, with $a = 500k_0$. Clearly they support the above analysis. It is interesting that the ratios $\langle \log(\kappa/a) \rangle / \langle \log \xi \rangle = 2$ and $\langle (\log(\kappa/a))^2 \rangle_c / \langle (\log \xi)^2 \rangle_c = 7$ are more accurately maintained than the absolute values predicted by the short-time approximation. It may be that the ratios hold for some more basic reason, though we do not know what it is.

For longer times the pattern of time dependence for the log-cumulants of the curvature that was established for the two-dimensional case is effectively repeated in three dimensions for the curvature of line elements. The results for the first six moments with an initial value of zero for the curvature are shown in figure 5. Completely identical limiting results are achieved with any value for the initial curvature. Of course the detailed analysis is somewhat different since the very close

relationship between stretching and curvature suppression is not repeated. As noted above for line elements in three dimensions (Ishihara & Kaneda 1992) we cannot use incompressibility of the flow to infer the same close connection between stretching and curvature suppression as exists in two dimensions. Nevertheless the quantity $A(t)$ must have statistical properties in three dimensions similar to the corresponding quantity in two. We will see in the following section that the propensity of $A(t)$ to acquire negative values, which at least qualitatively is associated with periods of contraction for the material element in question, inevitably implies the existence of a power-law tail in the probability distribution for the curvature with the consequence that certain moments of the curvature diverge even though the moments or cumulants of the log-curvature remain finite.

5. Stochastic model of the curvature equations

In order to understand the way in which (30) gives rise to a power-law tail for the curvature distribution it is illuminating to model the equation by means of a stochastic differential equation in which $A(t)$ and $B(t)$ are represented by stochastic processes. Such an equation has been investigated in Drummond (1992). For our purposes it is sufficient to proceed in the following way. We introduce a stochastic process $y(t)$ which takes values in a vector space (possibly one-dimensional). The coefficients A and B are then thought of as being functions of $y(t)$. The process $y(t)$ which is assumed to be stationary in time is characterized by a probability distribution $P_0(y)$ and a correlation time τ . If we define the statistical ‘Laplacian’ for y to be Δ , where

$$\Delta f(y) = \lim \left\{ \frac{1}{h} E[f(y(t+h)) - f(y(t)) | y(t) = y] \right\} \quad \text{as } h \rightarrow 0, \quad (44)$$

where $E[X|Y]$ means the expected value of X subject to the condition Y , then the probability distribution $P_0(y)$ satisfies

$$\Delta^\dagger P_0(y) = 0, \quad (45)$$

where Δ^\dagger is the Hermitian conjugate operator to Δ . The theory of Markovian stochastic differential equations tells us that (30) implies that $P(y, \kappa)$, the stationary joint distribution of y and κ (if it exists), satisfies

$$\Delta^\dagger P(y, \kappa) + \frac{\partial}{\partial \kappa} (A(y) \kappa - B(y)) P(y, \kappa) = 0. \quad (46)$$

We now specialize to models in which y holds its value for discrete time intervals. Models of this kind have been studied more extensively in Drummond (1992). At any given point in time the value of y changes with a constant probability per unit time. This means that the lengths of the time intervals are distributed according to the Poisson distribution. We assume the mean length of a time interval is τ . Within a time interval the probability distribution of y is $P_0(y)$, the values of y in distinct intervals being independently distributed. Under these circumstances it is easy to show that

$$\Delta f(y) = \frac{1}{\tau} \left(\int dy' P_0(y') f(y') - f(y) \right), \quad (47)$$

and
$$\Delta^\dagger f(y) = \frac{1}{\tau} \left(P_0(y) \int dy' f(y') - f(y) \right). \quad (48)$$

In the interests of generating simple models that are easily investigated either by analytical or numerical methods we specialize further and assume that y takes on only a finite number of discrete values $\{y_n\}$, $n = 1, 2, \dots, N$ with corresponding probabilities $\{q_n\}$. That is $y(t)$ is a discrete Markov chain in continuous time. We set $A(y_n) = a_n$ and $B(y_n) = b_n$. The joint probability distribution becomes $p_n(\kappa)$ and satisfies the equivalent of (46), namely

$$\frac{1}{\tau}(\mathbf{q}\mathbf{u}^T - \mathbf{I})\mathbf{p} + \frac{\partial}{\partial \kappa}(\kappa\mathbf{A} - \mathbf{B})\mathbf{p} = 0, \tag{49}$$

where we have used a matrix notation in which

$$\mathbf{p} = \begin{pmatrix} p_1(\kappa) \\ p_2(\kappa) \\ \vdots \end{pmatrix}, \quad \mathbf{q} = \begin{pmatrix} q_1 \\ q_2 \\ \vdots \end{pmatrix}, \quad \mathbf{u} = \begin{pmatrix} 1 \\ 1 \\ \vdots \end{pmatrix}, \tag{50}$$

and

$$\mathbf{A} = \begin{pmatrix} a_1 & & \\ & a_2 & \\ & & \ddots \end{pmatrix}, \quad \mathbf{B} = \begin{pmatrix} b_1 & & \\ & b_2 & \\ & & \ddots \end{pmatrix}. \tag{51}$$

In order to achieve a completely explicit model we analyse the case of two components, with $a_1 = \gamma$, $a_2 = \rho$, $b_1 = \beta$, and $b_2 = -\beta$. We will also assume that $q_1 = q_2 = \frac{1}{2}$. The equations for $p_1(\kappa)$ and $p_2(\kappa)$ become

$$\frac{d}{d\kappa} \begin{pmatrix} \gamma\kappa - \beta & 0 \\ 0 & \rho\kappa + \beta \end{pmatrix} \begin{pmatrix} p_1(\kappa) \\ p_2(\kappa) \end{pmatrix} = \frac{1}{2\tau} \begin{pmatrix} 1 & -1 \\ -1 & 1 \end{pmatrix} \begin{pmatrix} p_1(\kappa) \\ p_2(\kappa) \end{pmatrix}. \tag{52}$$

The analysis of this equation is not difficult, and it is easily checked that the solution has the analytical form

$$\begin{pmatrix} p_1(\kappa) \\ p_2(\kappa) \end{pmatrix} \propto \begin{pmatrix} (\gamma\kappa - \beta)^{a-1} (\rho\kappa + \beta)^b \\ -(\gamma\kappa - \beta)^a (\rho\kappa + \beta)^{b-1} \end{pmatrix}, \tag{53}$$

where $a = 1/2\tau\gamma$ and $b = 1/2\tau\rho$. In order to obtain the precise form of the probability distribution it is necessary to take into account the signs of the various parameters. There is no loss of generality in assuming that $\beta > 0$. If now we assume that $\gamma > 0$ and $\tau > 0$ then it is clear from (30) that in the range $\kappa > \beta/\gamma$, $\dot{\kappa} < 0$ and in the range $\kappa < -\beta/\rho$, $\dot{\kappa} > 0$. That is, in both cases κ moves towards the region $-\beta/\rho < \kappa < \beta/\gamma$. Once κ is inside this range $\dot{\kappa}$ can fluctuate in sign. In the limit of large times when the support for the probability distribution for κ will be confined to this range. Taking into account the positivity and correct normalization of the probability distributions we find for $-\beta/\rho < \kappa < \beta/\gamma$

$$\begin{pmatrix} p_1(\kappa) \\ p_2(\kappa) \end{pmatrix} = C^{-1} \begin{pmatrix} (\beta - \gamma\kappa)^{a-1} (\beta + \rho\kappa)^b \\ (\beta - \gamma\kappa)^a (\beta + \rho\kappa)^{b-1} \end{pmatrix}, \tag{54}$$

where

$$C = 2\gamma^{a-1}\rho^{b-1} \left(\frac{1}{\gamma} + \frac{1}{\rho}\right)^{a+b-1} \beta^{a+b} \frac{\Gamma(a)\Gamma(b)}{\Gamma(a+b)}. \tag{55}$$

For κ outside this range the probability distributions vanish identically for the reasons indicated above. The total probability distribution for κ is $P(\kappa = p_1(\kappa) + p_2(\kappa)$.

The interpretation of these results in terms of our original problem is that in circumstances, were they to exist, where the stretching coefficient $A(t)$ remains positive

throughout its fluctuating history, the curvature distribution would be sharply suppressed for large values of the curvature and all moments of the curvature would settle down to finite values. A more realistic assumption is that $A(t)$ can fluctuate to negative values. We can mimic this effect by setting $\gamma = -\alpha$ where $\alpha > 0$. Under these circumstances the nature of the curvature probability distribution changes radically. We can understand what happens by moving γ continuously from positive to negative values. As γ passes through zero, two things happen simultaneously. First the upper end of the support range for the probability distribution reaches infinity and passes through it to attain negative values. Second the power of the singularity in the analytic form of the probability distribution at this displaced ‘end point’ ceases to be integrable. We have from (53)

$$p_1(\kappa) \sim (\beta + \alpha\kappa)^{-\frac{1}{2\tau\alpha}-1}. \tag{56}$$

This is clearly non-integrable. The resolution of the difficulty is that infinity takes over the role of the displaced end point and the support range for the probability distribution becomes $-\beta/\rho < \kappa < \infty$. The reason that this is possible is that the singularity of the analytic form of the distribution at $\kappa \sim \infty$ has now become integrable. From (53) we see that

$$p_1(\kappa) \sim p_2(\kappa) \sim \kappa^{b-c-1}, \tag{57}$$

where $c = 1/2\tau\alpha$. In its new form of the probability distribution vanishes for $\kappa < -\beta/\rho$, while for $\kappa > -\beta/\rho$ it is given by

$$\begin{pmatrix} p_1(\kappa) \\ p_2(\kappa) \end{pmatrix} = C'^{-1} \begin{pmatrix} (\beta + \alpha\kappa)^{-c-1} (\beta + \rho\kappa)^b \\ (\beta + \alpha\kappa)^{-c} (\beta + \rho\kappa)^{b-1} \end{pmatrix}, \tag{58}$$

where
$$C' = 2\alpha^{-c} \rho^{b-1} \beta^{b-c} \left(\frac{1}{\alpha} - \frac{1}{\rho}\right)^{b-c} \frac{\Gamma(b)\Gamma(c-b)}{\Gamma(c)}. \tag{59}$$

To mimic a situation in which $\langle A(t) \rangle > 0$ we require $\alpha < \rho$, thus ensuring that $c > b$ and hence the integrability of the infinite end point. If in a rather unphysical way, this condition were broken then we would conclude that there was no stationary distribution for κ and the associated κ -diffusion process would result in all material elements becoming infinitely curved! Rejecting this possibility we find that the consequence of the intermittent reversal of sign of $A(t)$ is the appearance of a power-law tail in the curvature distribution as indeed seems to be borne out in the results of numerical simulations.

We can see how distributions of the kind resulting from the above stochastic model can lead to the features observed for the moments and cumulants of the logarithm of the curvature in various simulations. (Where appropriate we will interpret κ to mean $|\kappa|$.) For example we could make a very crude model for the distribution of κ along the following lines. Set

$$P(\kappa) \propto \begin{cases} 1, & 0 < \kappa < 1 \\ 1/\kappa^{-\lambda-1}, & 1 < \kappa < \infty. \end{cases} \tag{60}$$

The choice of $\kappa = 1$ as the splitting point between the body and tail of the distribution is arbitrary and only made for the purposes of illustration. With this model distribution we can calculate the moments of $\log \kappa$ to obtain

$$\langle (\log \kappa)^p \rangle = \Gamma(p+1) \frac{(-1)^p + \lambda^{-p-1}}{1 + \lambda^{-1}}. \tag{61}$$

We see then there are two contributions to $\langle(\log \kappa)^p\rangle$ both of which increase rapidly with p . That from the body of the distribution alternates in sign while that from the tail is positive and for sufficiently small $\lambda = c - b$ will dominate at large p . If we assume this dominance of the tail then we find

$$\langle(\log \kappa)^p\rangle/\langle(\log \kappa)^{p-1}\rangle = p/\lambda. \quad (62)$$

Of course it is not clear where in practice this asymptotic ratio sets in. This is an interesting problem in its own right both for the stochastic model and the original flow simulations themselves. However if we examine the numerical results for the line element log-curvature in three dimensions we find

$$\langle(\log \kappa)^6\rangle:\langle(\log \kappa)^5\rangle:\langle(\log \kappa)^4\rangle:\langle(\log \kappa)^3\rangle = 1280:175:31:6.15$$

suggesting a value $\lambda = 0.83 \pm 0.05$. The value of the corresponding quantity for surface elements measured by Pope *et al.* (1989) was 0.55.

The simple stochastic model discussed above is very useful because it can be solved in such an explicit fashion. However it is rather too simple in that it forces a correlation between the stretching and bending terms that is unrealistic. This is why the power-law tail occurs only for positive κ . It is easy to build more complex models not subject to such constraints (Drummond 1992) that exhibit the same properties.

6. Conclusions

In this paper we have shown that the exponential increase of the powers of material line elements in random flows can be understood in terms of the cumulant expansion of the logarithm of the line element length. This is a generalization of Kraichnan's approach in which he examined the behaviour of line elements in the Markovian limit of random flows. Our approach not only shows that the result can hold even when the Markovian limit is not appropriate it also shows that circumstances can arise in which the result may not hold. These circumstances typically involve correlations of anomalously long range in time for the log-length of the line elements. We illustrate the occurrence of such a situation by using a flow field ensemble for which the Gaussian statistics are severely broken.

The version of the Pope (1988) equation appropriate to the time development of curvature in material line elements (Drummond & Münch 1991) was examined in detail. For the case of two-dimensional flow the connection between element stretching and curvature suppression is particularly close. We were able to confirm this relationship directly in the simulation. In three dimensions the relationship is slightly more indirect, nevertheless it is qualitatively similar. There can be no doubt about the correctness of the Pope equation. Its implications for the probability distribution of the relevant curvature quantities was further explored by modelling the equation as a stochastic differential equation (Drummond 1992). We showed explicitly in a simple case that the power-law tail for the probability distribution of curvature is indeed the consequence of events in which the material element shrinks rather than expands. This is consistent not only with the anti-correlation of curvature production and expansion observed by Drummond & Münch (1991) but also with the observations of Pope *et al.* (1989) of the power-law tail in simulation studies and the discovery by Girimaji (1991) of the finiteness of moments of the log-curvature of surface elements. In this paper we confirmed that in two and three dimensions the moments of the log-curvature of line elements also stabilizes at a finite value for large times.

The conclusion from the above is that the nature of curvature generation for

material elements in random flows or turbulence is reasonably well understood. There are some obvious ways in which the studies can be taken further. Clearly these methods, both simulation and theory, can be applied to deterministic but chaotic flow studies which are the basis of much thinking on mixing in flows. The preliminary work on torsion production in line elements (Drummond & Münch 1991), of importance to magnetic field behaviour (Moffatt 1978; Drummond, Duane & Horgan 1986) merits further investigation for random, turbulent and deterministic flows. A remaining question is the implication for the global behaviour of lines and surfaces in random flows, of the local results so far obtained. For example, the power-law tail in the curvature distribution must have something to reveal about the nature and frequency of fold-hinges in the history of lines and surfaces in a mixing flow.

REFERENCES

- ARNOLD, L., KLIEMANN, W. & OELJEKLAUS, E. 1985 Lyapunov exponents. In *Lyapunov Exponents* (ed. L. Arnold & V. Wihstutz), pp. 85–125. Lecture Notes in Mathematics. Springer.
- BACHELOR, G. K. 1952 The effect of homogeneous turbulence on material lines and surfaces. *Proc. R. Soc. Lond. A* **213**, 349.
- COCKE, W. J. 1969 Turbulent hydrodynamic line stretching: consequences of isotropy. *Proc. R. Soc. Lond. A* **213**, 349.
- DRUMMOND, I. T. 1992 Multiplicative stochastic differential equations with noise induced transitions. *J. Phys. A: Math. Gen.* **25**, 2273.
- DRUMMOND, I. T., DUANE, S. & HORGAN, R. R. 1984 Scalar diffusion in simulated helical turbulence with molecular diffusivity. *J. Fluid Mech.* **138**, 75.
- DRUMMOND, I. T., DUANE, S. & HORGAN, R. R. 1986 Numerical simulation the α -effect and turbulent magnetic diffusion with molecular diffusivity. *J. Fluid Mech.* **163**, 425.
- DRUMMOND, I. T. & MÜNCH, W. 1990 Turbulent stretching of line and surface elements. *J. Fluid Mech.* **215**, 45.
- DRUMMOND, I. T. & MÜNCH, W. 1991 Distortion of line and surface elements in model turbulent flows. *J. Fluid Mech.* **225**, 529.
- GIRIMAJI, S. S. 1991 Asymptotic behavior of curvature of surface elements in isotropic turbulence. *Phys. Fluids A* **3**, 1771.
- ISHIHARA, T. & KANEDA, Y. 1992 Stretching and distortion of material line elements in two-dimensional turbulence. *J. Phys. Soc. Japan* **61**, 3547.
- KRAICHNAN, R. H. 1970 Diffusion by a random velocity field. *Phys. Fluids* **13**, 22.
- KRAICHNAN, R. H. 1974 Convection of a passive scalar by a quasi-uniform random straining field. *J. Fluid Mech.* **64**, 737.
- MOFFATT, H. K. 1978 *Magnetic Field Generation in Electrically Conducting Fluids*. Cambridge University Press.
- ORSZAG, S. A. 1970 Comments on 'Turbulent hydrodynamic line stretching: consequences of isotropy'. *Phys. Fluids* **13**, 2203.
- OTTINO, J. M. 1989 *Kinematics of Mixing: Stretching, Chaos and Transport*. Cambridge University Press.
- OTTINO, J. M. 1990 Kinematics of chaotic mixing: experimental and computational results. In *Topological Fluid Mechanics* (ed. H. K. Moffatt & A. Tsinober). Cambridge University Press.
- POPE, S. B. 1988 The evolution of surfaces in turbulence. *Intl J. Engng Sci.* **26**, 445.
- POPE, S. B., YEUNG, P. K. & GIRIMAJI, S. S. 1989 The curvature of material surfaces in isotropic turbulence. *Phys. Fluids A* **1**, 2010.
- PRESS, W. H., FLANNERY, B. P., TEUKOLSKY, S. A. & VETTERLING, W. T. 1986 *Numerical Recipes*. Cambridge University Press.
- VASSILICOS, J. C. & HUNT, J. C. R. 1992 Turbulent flamelet propagation. *Combust. Sci. Tech.* **87**, 291.